A Stability Diagram Computation Method for Milling Adapted to Automotive Industry

Jean Vincent LE LAN, Audrey MARTY, Jean-François DEBONGNIE
Jean-Vincent LE LAN, API FR CTR B02 1 60, Renault SAS, 67 rue des Bons raisins, 92508 Rueil Malmaison CEDEX, France
jean-vincent.le-lan@renault.com

Abstract: In this paper, a numerical method to compute stability diagrams is presented. It is adapted to the particular case of automotive parts production where chatter arises due to the lack of stiffness of the workpiece. The main features of the model are the simultaneous immersion of many teeth, frequency domain computations and the use of the Finite Element Method to provide transfer function.
Keywords: Chatter, FEM, Milling

1. INTRODUCTION

Chatter is due to self-generative vibrations that occur when the chip width is too great versus dynamic stiffness [Tlusty ,1999]. This phenomenon leads to a bad surface aspect and a high noise level. It also reduces tool life and consequently increases production costs. For instance, the cost due to chatter on a recent cylinder block is estimated to be around 0.35€ per piece. As Renault S.A.S. produces around 3 million engines per year, the avoidance of chatter becomes strategic.
In this context, Renault's powertrain division decided to focus on predicting chatter. As the resulting method is to be used on early stages of process planning, it has been decided to use FEM to predict the dynamic behavior of workpieces.
A first attempt was to use the criterion proposed by Tlusty and Polacek in 1957 [Tlusty *et al.*, 1957]. This criterion has been successfully adapted to turning for automotive industry where workpieces are generally more compliant than the tool. Then Masset and Belluco extended the method successfully to milling [Masset *et al.*, 2004].
However, the Masset-Belluco method is not valid when more than one tooth is immersed and it does not provide any stability diagram corresponding to Tobias criterion [Tobias *et al.*, 1958].
On another hand, Altintas and Budak have proposed a method to compute a stability diagram that corresponds to Tobias' chatter maps in 1995 [Altintas *et al.*, 1995] but it does not apply to automotive industry cases because it focuses on a compliant tool. Another attempt of the same team focuses on taking into account the dynamic behaviour of the workpiece through the use of compliance-damping systems in two directions [Budak *et al.*, 1998 1,2].

This work is based on the Altintas-Budak theory. It is an adaptation of this theory to vibrating workpieces and is used to extend the Masset-Belluco results to multiple immerged teeth and to a stability diagram computation. It computes stability limits at each machined surface nodes using both tool and machined surface compliance expressed at each nodes. It can also be seen as an adaptation of the work presented in [Budak *et al.*, 1998 1] where the compliance-damping systems representing the workpiece is evolving along the positions of the tool.

2. COMPUTATION METHOD

2.1. An adaptation of the Altintas-Budak method for a single immersed tooth

The method presented in this paper is an adaptation of the Altintas-Budak method [Altintas *et al.*, 1995] to the cases encountered in the automotive industry, where machining operations, specifically milling, are run with machine tools that are much stiffer in comparison to workpieces. This leads to chatter cases which are due to an excessive compliance of the workpiece while the Altintas-Budak method focuses on vibrating tools.

Cutting forces applied on the workpiece by an immersed tooth labelled j and due to vibrations can be formulated as:

$$\begin{aligned} dF_{t,j} &= K_t b h(\phi_j) \\ dF_{r,j} &= K_r dF_{t,j} \\ dF_{a,j} &= K_a dF_{t,j} \end{aligned} \quad . \qquad (1)$$

Here, coefficients K_x, $x = t,r,a$, are respectively representing cutting pressures used in the linear cutting force model and two dimensionless coefficients. These coefficients are obtained through a derivation of Kienzle's model.

Furthermore, b represents the chip width, h, the chip thickness and ϕ_j, the angular position of tooth j.

These cutting forces, as expressed in the tooth coordinate system, have to be transformed in the wokpiece coordinate system through two rotations (figure 1).

This leads to the following expression of the cutting forces in the workpiece coordinate system:

$$\underline{F}(t) = \begin{bmatrix} dF_x \\ dF_y \\ dF_z \end{bmatrix} = bK_{t,j} \underline{\underline{A}} \begin{bmatrix} dx \\ dy \\ dz \end{bmatrix} = bK_{t,j} \underline{\Delta}(t) , \qquad (2)$$

where matrix $\underline{\underline{A}}$ contains the two rotations and the cutting forces coefficients. This matrix is valid in the time domain when a studied node of the machined surface is cut.

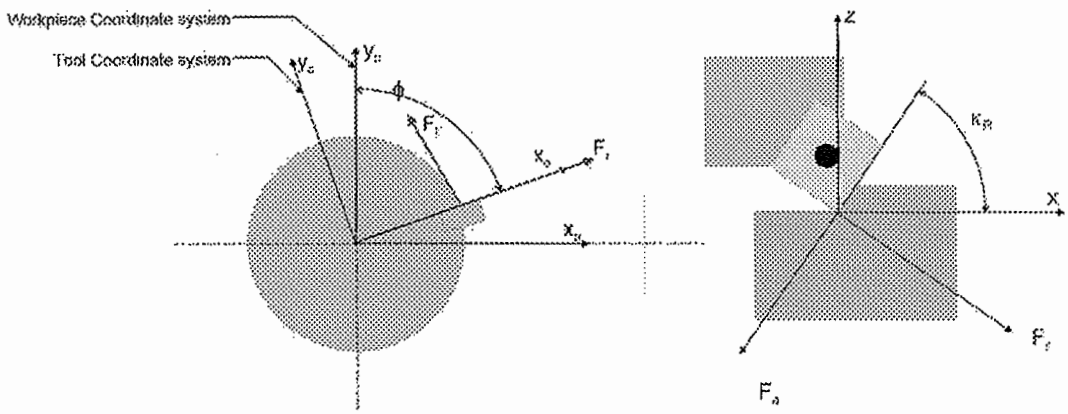

Figure 1; The two rotations. κ_R is the tool working cutting edge angle.

In Laplace's domain, the average value of $\underline{\underline{A}}$, namely $\underline{\underline{A}}_0$ is used:

$$\underline{\underline{A}}_0 = \frac{Z}{4\pi}\underline{\underline{A}}, \tag{3}$$

where Z is the number of teeth of the tool.
Finally, the expression of cutting forces in Laplace's domain is:

$$\underline{F}(s) = bK_t\underline{\underline{A}}_0\underline{\Delta}(s). \tag{4}$$

The complete system can be summarized in a bloc diagram as done in figure 2. This representation shows the effect of the transfer functions of the mechanical system which connects displacements of the tool with cutting forces. These transfer functions are contained in the transfer function matrix $\underline{\underline{\Psi}}(i\omega)$.

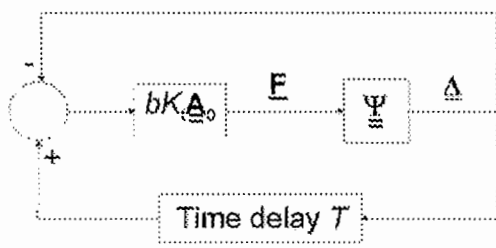

Figure 2; Bloc diagram of the system.

In the approach presented here, the transfer function matrix is computed using FEM. Considering the time-delay T between two teeth, this leads to:

$$\underline{\Delta}(i\omega_c) = \left[1 - e^{-i\omega_c T}\right]\underline{\underline{\Psi}}(i\omega_c)\underline{F}(i\omega_c) \tag{5}$$

at a chosen chatter pulsation ω_c.
This last equation and equation (4) are leading to the eigenvalue problem:

$$\det\left[\underline{\underline{I}} - \Lambda\underline{\underline{\Psi}}_0(i\omega_c)\right] = 0, \tag{6}$$

where:

$$\Lambda = \frac{-Z}{4\pi} bK_t\left(1-e^{i\omega_c T}\right)$$
$$\underline{\underline{\Psi}}_0 = \frac{4\pi}{Z}\underline{\underline{A}}_0\underline{\underline{\Psi}}(i\omega_c) \tag{7}$$

Solving problem (6) for chosen chatter pulsations leads to a limit chip width b_{lim} for each ω_c:

$$b_{\text{lim}} = \frac{2\pi \text{Re}(\Lambda)}{ZK_t}\left(1+\kappa^2\right), \tag{8}$$

where $\kappa = \frac{\text{Im}(\Lambda)}{\text{Re}(\Lambda)}$.

As a spindle speed N excites many harmonics, each b_{lim} corresponds to many spindle speeds given as:

$$N = \frac{60\omega_c}{Z\left(\varepsilon + 2k\pi\right)} \text{ in R.P.M. }, \tag{9}$$

where:

$$\varepsilon = \pi - 2\arctan(\kappa) \tag{10}$$

and k is an integer.

2.2. Immersion of multiple teeth

The original Altintas-Budak method considers multiple immerged teeth but it is not suited for compliant workpieces because it implicitly assumes that two nodes simultaneously cut have the same dynamic behaviour.

In order to correct this feature, the dynamic behaviour of each cut node and the interactions between nodes have to be taken into account.

Considering n simultaneously immerged teeth, the cutting forces for tooth i, as already seen, become:

$$\underline{F}_i(s) = bK_t\underline{\underline{A}}_{0,i}\underline{\Delta}_i(s) \tag{11}$$

and the displacement of the tooth is given by

$$\underline{\Delta}_i(i\omega_c) = \left[1-e^{-i\omega_c T}\right]\sum_{j=1}^{n}\left(\underline{\underline{\Psi}}_{ij}(i\omega_c)\underline{F}_j(i\omega_c)\right), \tag{12}$$

where matrices $\underline{\underline{\Psi}}_{ij}$ contain the transfer functions between a force applied on node i and the resulting displacement of node j.

Using the same method as explained for the single immersed tooth case, the research of stability limit results in solving the following eigenvalue problem:

$$\det\left(\underline{\underline{I}}+\Lambda\begin{bmatrix}\underline{\underline{A}}_{0,1} & \cdots & 0 & \cdots & 0\\ \vdots & \ddots & \vdots & & \vdots\\ 0 & \cdots & \underline{\underline{A}}_{0,i} & & 0\\ \vdots & & & \ddots & \vdots\\ 0 & \cdots & 0 & \cdots & \underline{\underline{A}}_{0,n}\end{bmatrix}\begin{bmatrix}\underline{\underline{\Psi}}_{11} & \cdots & \underline{\underline{\Psi}}_{1i} & \cdots & \underline{\underline{\Psi}}_{1n}\\ \vdots & & \vdots & & \vdots\\ \underline{\underline{\Psi}}_{i1} & \cdots & \underline{\underline{\Psi}}_{ii} & \cdots & \underline{\underline{\Psi}}_{in}\\ \vdots & & \vdots & & \vdots\\ \underline{\underline{\Psi}}_{n1} & \cdots & \underline{\underline{\Psi}}_{ni} & \cdots & \underline{\underline{\Psi}}_{nn}\end{bmatrix}\right)=0\,. \qquad (13)$$

As the global problem is expressed in three dimensions, there are $3n$ eigenvalues for Λ leading to chip widths. Only the smallest chip width is kept for each chatter pulsations.
In some cases, the tool and the workpiece are both compliant. In order to solve such cases, both behaviours (tool and workpiece) have to be taken into account. Following [Bravo *et al.*, 2005], transfer matrices of tool and workpiece have to be summed. This leads to the following expression:

$$\det\left(\underline{\underline{I}}+\Lambda\begin{bmatrix}\underline{\underline{A}}_{0,1} & \cdots & 0 & \cdots & 0\\ \vdots & \ddots & \vdots & & \vdots\\ 0 & \cdots & \underline{\underline{A}}_{0,i} & & 0\\ \vdots & & & \ddots & \vdots\\ 0 & \cdots & 0 & \cdots & \underline{\underline{A}}_{0,n}\end{bmatrix}\begin{bmatrix}\underline{\underline{\Psi}}^{w}_{11}+\underline{\underline{\Psi}}^{t}_{11} & \cdots & \underline{\underline{\Psi}}^{w}_{1i}+\underline{\underline{\Psi}}^{t}_{1i} & \cdots & \underline{\underline{\Psi}}^{w}_{1n}+\underline{\underline{\Psi}}^{t}_{1n}\\ \vdots & & \vdots & & \vdots\\ \underline{\underline{\Psi}}^{w}_{i1}+\underline{\underline{\Psi}}^{t}_{i1} & \cdots & \underline{\underline{\Psi}}^{w}_{ii}+\underline{\underline{\Psi}}^{t}_{ii} & \cdots & \underline{\underline{\Psi}}^{w}_{in}+\underline{\underline{\Psi}}^{t}_{in}\\ \vdots & & \vdots & & \vdots\\ \underline{\underline{\Psi}}^{w}_{n1}+\underline{\underline{\Psi}}^{t}_{n1} & \cdots & \underline{\underline{\Psi}}^{w}_{ni}+\underline{\underline{\Psi}}^{t}_{ni} & \cdots & \underline{\underline{\Psi}}^{w}_{nn}+\underline{\underline{\Psi}}^{t}_{nn}\end{bmatrix}\right)=0\,, \qquad (14)$$

where indices t and w are respectively marking transfer matrices of the tool and of the workpiece.

2.3. Condition of use

The method is valid only if the regenerative effect is effective i.e. if the modulation left by the previous teeth in the neighbourhood of the studied node affects the tool. A sufficient condition for the validity of the method is that the wavelength of chatter modulation has to be smaller than the distance between two nodes.
This condition is sufficient but not necessary.

2.4. Computation details

The computation method consists in choosing a node on the machined surface and finding the stability diagram for this node. When the chosen node is cut the positions of the other immerged teeth are not necessarily corresponding to existing nodes but are contained in triangular elements as shown in figure 3.
Therefore, transfer functions of these positions are computed as a linear combination of the three nodes of the element using shape functions. Generating matrices for two different indices (for instance A and B) implies computing a lot of transfer functions. Therefore, it is of paramount importance to organize the computation so that it is not too time-consuming.

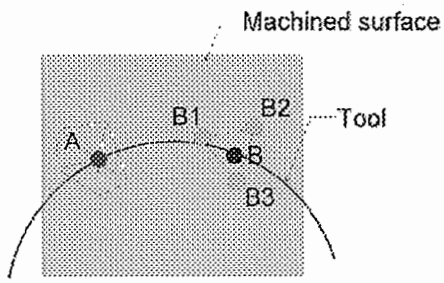

Figure 3; A is the studied node, the second immerged teeth B does not correspond to any node of the machined surface. Therefore, its behaviour is composed of B1 B2 and B3's behaviour using the shape functions of the element in which it is situated.

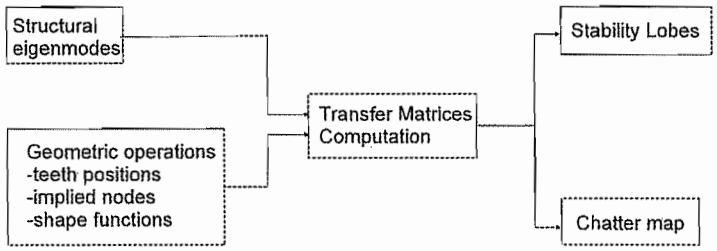

Figure 4; General organisation of the computing method.

3. APPLICATION ON A CYLINDERBLOCK

The milling of one face of the crankcase of the new Renault's 2.0l dCi diesel engine (130 kW, 360 Nm @ 2000 RPM, Euro 4) is presented. The crankcase was originally developed to be mass optimized for its functionality, which resulted in several compliant surfaces, difficult to face mill.

3.1. Process setup

A scheme of the process set-up is shown in figure 5. It is possible to mill the surface in two passes within the assigned cycle time in order to decrease the depth of cut to 1.5 mm.

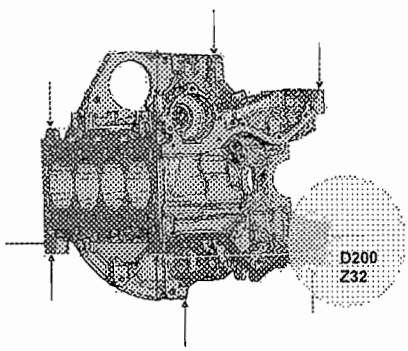

Tool diameter	200 mm
Spindle speed	250 RPM
Feed	1900 mm/min
Number of teeth	32
Tool working cutting edge angle	45°
Depth of cut	3 mm

Figure 5; Machined surface, clamping system, tool and cutting conditions.

3.2. Application of the method

Transfer function matrices computation

In order to avoid errors due to the truncation of the basis of the solution space, eigenvectors of the structure are computed up to two times the maximal frequency of the study.

In this case, the chosen maximal frequency of the study is 4.5 kHz so the 247 eigenvectors corresponding to eigenfrequencies lower than 9kHz are computed. Figure 6 presents a transfer function and the eigenvector corresponding to the predominant mode.

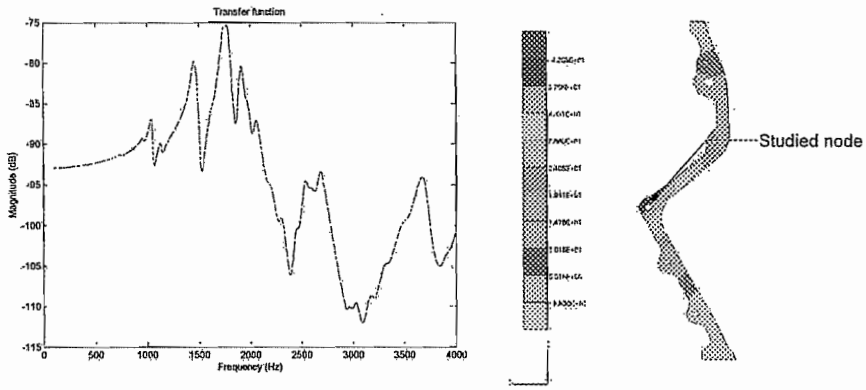

Figure 6; Transfer function between a node and itself in the direction normal to the machined surface and the predominant mode eigenvector (1774 Hz).

Validation of the sufficient condition

The frequency of the predominant mode is 1774 Hz. Therefore, the chatter frequency is around 1774 Hz. If a maximal spindle speed around 500 RPM is considered, it gives a tooth speed of 5236 mm/s. The wavelength becomes equal to 2.91 mm this is less than the size of the mesh that is around 10 mm

Stability lobes computation

As tests exhibit chatter zones on the extreme left part of the machined surface, it has been decided to plot stability lobes for a node in this area. The flexibility of the tool is here neglected as the tool is very massive and from far more rigid than the workpiece.

The first step is to identify a node and to deduce the other immersed teeth and their respective angular positions as shown in figure 7 left.

Figure 7 right shows the maximum depth of cut usable in terms of stability versus the spindle speed. The difference between the two plots is that, for the single immersed tooth, only one node behaviour is taken into account while, in the multiple immersed teeth plot, both nodes behaviour are considered

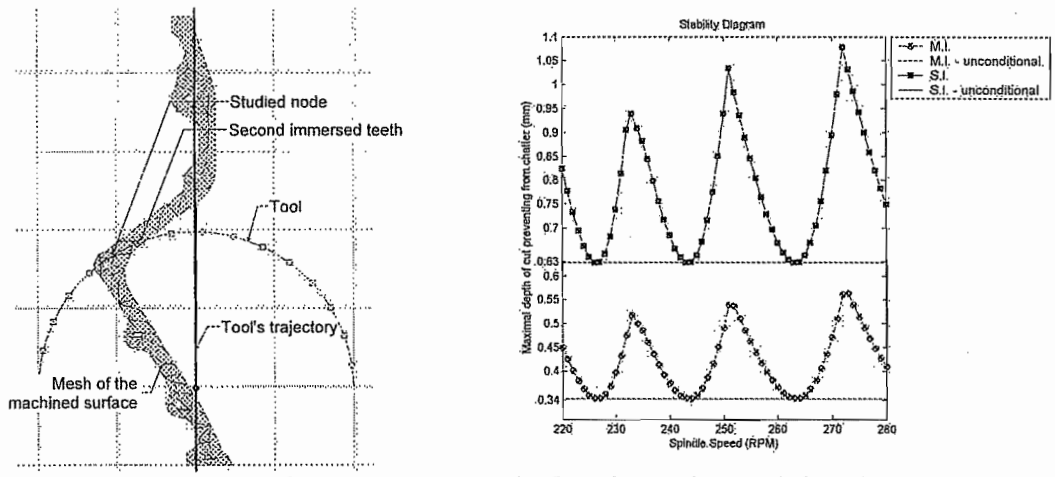

Figure 7; left: identification of the studied node. Right: Stability diagram for the two immerged teeth (MI) or with only the teeth on the studied node (SI).

Some remarks can be done:

- If the surface is milled with the presented trajectory, there will be some chatter near the studied node;
- In that case, the nodes are very near and presenting a similar behaviour implying no phase shift between the single immersed tooth plot and the multiple immersed teeth plot.
- Ignoring the second immersed teeth leads to an important error which could be harmful as giving too optimistic predictions.

Chatter map.

As can be seen, the lobes in the stability diagram are very close to each other because of low spindle speeds. Therefore, the fundamental information given by the diagram is the unconditional depth of cut, that prevents from chatter at any spindle speed. The computation of such depth of cut can be done on every node of the machined surface and a colormap can be plotted as done in figure 8.

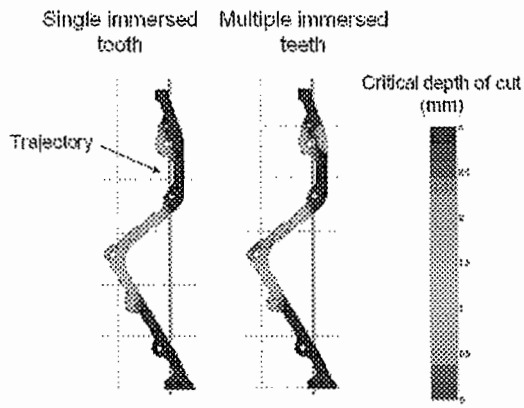

Figure 8; Chatter maps computed with the single immerged tooth hypothesis and the multiple immerged teeth method.

Comparison with tests

Tests have been conducted as specified in the process setup but varying the depth of cut. Figure 9 left presents a test part that has been face-milled with a 3mm depth of cut. As chatter zones are difficult to spot on the picture they have been circled in red.

Figure 9 right presents the result obtained using the presented method. Whereas the chatter zones are quite hard to spot on the part and the parameters are not well known, this first attempt shows encouraging results. Further work is to determine accurately cutting coefficients and use a microphone during the operation in order to localise chatter zones with precision.

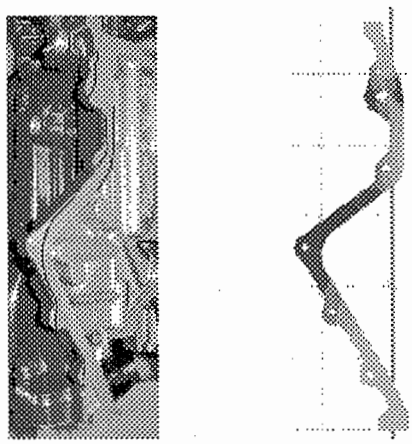

Figure 9; left: A test part. The operation has been run with a 3 mm depth of cut. Chatter zones are delimited by red lines. Right: The computed chatter map.

Computation time

The computation of both stability diagram and chatter map is done in two steps. The first step consists in finding the eigenmodes of the workpiece and, optionally, of the tool with a commercial FEM solver. For the presented example, this has been done on a shared calculator (IBM p655 84 processors 336 GO RAM and 9 TO hard drive) in 3200s for around 250000 nodes in the mesh of the global workpiece. Post-Treatment computations to deduce stability diagram takes 60s and chatter maps computation needs 90s.

Guaranteeing short computation time makes the use of FEM chatter prediction a useful tool for early stages of process planning when the final geometry of the workpiece may vary.

This way, the optimum workpiece design can be found which meets the demands for mass reduction and which insures enough rigidity for stable machining.

4. CONCLUSION

The present method for computing stability diagrams and chatter maps appears to be well adapted to automotive industry. In particular, stability diagrams are used for solving chatter problems on existing machine tools through slight modifications of spindle speeds. Chatter maps are more efficient in process planning when the problem is to choose efficient clamping devices and cutting parameters. They also facilitate collaborative negotiations between process planners and product designers.
This paper has shown that forgetting the multiple immersions of teeth could lead to a non-conservative prediction of the depth of cut preventing from chatter.

REFERENCES

[Tlusty ,1999] Tlusty, J.; "Manufacturing Process and Equipment"; Prentice Hall, 2001

[Tlusty *et al.*, 1957] Tlusty, J.; Polacek, M.; "Beispiele der Behandlung der Selbsterregten Schwingung de Werkzeugmaschinen"; In: *3. Fokoma*; Vogel-Verlag Wuerzburg; 1957

[Masset *et al.*, 2004] Masset, L.; Debongnie, J.F.; Belluco, W.; "Chatter Maps for Process Design of Powertrain Components"; In: *Proceeding of the 7th CIRP International Workshop on Modelling of Machining Operation*, pp. 251-258; 2004

[Tobias *et al.*, 1958] Tobias, S.A., Fishwick, W.; "Theory of Regenerative Machine Tool Chatter"; In: *Engineer vol. 205*, pp 199; 1958

[Altintas *et al.*, 1995] Altintas, Y.; Budak, E.; "Analytical Prediction of Stability Lobes in Milling"; In: *Annals of the CIRP 44/1:357-362*; 1995

[Budak *et al.* , 1998 1] Budak, E.; Altintas, Y.; "Analytical Prediction of Chatter Stability in Milling – Part I: General Formulation"; In: *Transactions of the ASME, Journal of dynamic systems vol. 120 pp22-30*; 1998

[Budak *et al.* , 1998 2] Budak, E.; Altintas, Y.; "Analytical Prediction of Chatter Stability in Milling – Part II: Application of the General Formulation to Common Milling Systems"; In: *Transactions of the ASME, Journal of dynamic systems vol. 120 pp31-36*; 1998

[Bravo *et al.*, 2005] Bravo, U.; Altuzuzarra, O.; Lopez de Lacalle, L.N; Sanchez, J.A.; Campa, F.J.; "Stability Limits of Milling Considering the flexibility of the Workpiece and the Machine"; In: *International Journal of Machine Tools and Manufacture*; 2005